

# Numerical investigation for the impact of CO<sub>2</sub> geologic sequestration on regional groundwater flow

Hajime Yamamoto<sup>a</sup>, Keni Zhang<sup>b</sup>, Kenzi Karasaki<sup>b</sup>, Atsunao Marui<sup>c</sup>,

Hitoshi Uehara<sup>d</sup>, and Noriaki Nishikawa<sup>d</sup>

<sup>a</sup>Taisei Corporation, 344-1 Nase-cho Totsuka-ku, Yokohama 245-0051, Japan

<sup>b</sup>Lawrence Berkeley National Laboratory, 1 Cyclotron Road, Berkeley, CA 94720, USA

<sup>c</sup>National Institute of Advanced Industrial Science and Technology, 1-1-1, #7 Higashi, Tsukuba 305-8567, Japan

<sup>d</sup>Japan Agency for Marine-Earth Science and Technology, 3173-25 Showa-machi Kanagawa-ku, Yokohama 236-0001, Japan

## Abstract

Large-scale storage of carbon dioxide in saline aquifers may cause considerable pressure perturbation and brine migration in the deep formations, which may give rise to a significant influence on the regional groundwater system. With the help of parallel computing techniques, a comprehensive, large-scale numerical simulation of CO<sub>2</sub> geologic storage that predicts not only CO<sub>2</sub> migration but also its impact on regional groundwater flow was performed. As a case study, a hypothetical industrial-scale CO<sub>2</sub> injection in the Tokyo Bay, which is surrounded by the most industrialized area in Japan, was considered, and the impact of down-dip CO<sub>2</sub> injection on up-dip near-surface aquifers was investigated. A regional hydrogeological model with an area of about 60km×70km around the Tokyo Bay was discretized into about 10 million gridblocks. To solve the high-resolution model efficiently, we used a parallelized multiphase flow simulator TOUGH2-MP/ECO2N on a world-class high performance supercomputer in Japan, the Earth Simulator. In the simulation, CO<sub>2</sub> was injected into a storage aquifer at about 1km depths under the Tokyo bay from 10 wells with the total rate of 10 million tons/year for 100 years. Through the model, regional groundwater pressure build-up and seepage changes at land surface are examined. The results suggest that even if containment of CO<sub>2</sub> plume is ensured, pressure buildup in the order of tens of meters can occur in shallow confined layers of extensive regions including urban inlands.

*Keywords:* CO<sub>2</sub> storage; parallel computation, large-scale simulation; groundwater pressure; Tokyo Bay; Kanto Plain; Earth Simulator

## 1. Introduction

It is believed that the greenhouse gas may cause global climate change. One of the proposed approaches for reducing the greenhouse gas content in the atmosphere is through capturing CO<sub>2</sub> from large emission sources and injecting it into deep saline

aquifers. However, when a volume of CO<sub>2</sub> is injected into a virgin/native aquifer, it pushes the equivalent volume of water out of the aquifer. In industrial-scale projects of CO<sub>2</sub> geologic storage, it is expected that the amount of CO<sub>2</sub> fluid injected into an aquifer can be several million tons per year for a typical storage site. Continuous long-term injections for more than several decades will buildup groundwater pressures in extensive regions. Recently, it has been suggested that large-scale CO<sub>2</sub> injections may have a hydrological and geochemical impact on even shallow groundwater resources (Yamamoto et al., 2007; Birkholzer et al., 2008; Nicot, 2007). Birkholzer et al. (2008) conducted a sensitivity study on pressure response in radically symmetrical stratified systems. Nicot (2007) investigated the impact of a hypothetical large-scale injection on regional groundwater at the Texas Gulf Coast Basin using conventional groundwater flow models. Doughty and Pruess (2004) investigated physical processes that occur during the sequestration of CO<sub>2</sub> with site-scale models for the Frio pilot project. Several other recent studies (e.g. Ghomian et al. 2008) also investigated influence of CO<sub>2</sub> sequestration on regional groundwater, such as pressure build-up and CO<sub>2</sub> plume distribution. These studies all employed rather idealized representations of the geology with relatively small scale. However, influence of CO<sub>2</sub> sequestration may reach the whole regional groundwater basin.

During a Carbon dioxide storage process, CO<sub>2</sub> is injected in a supercritical state that has a much lower density and viscosity than the liquid brine it displaces. In situ, the supercritical CO<sub>2</sub> partitions between an immiscible gas-like phase and dissolution in the aqueous phase, involving complex multiphase flow processes as well as geomechanical, and geochemical processes, such as advection and diffusion, convective mixing, phase appearance/disappearance, dissolution and precipitation of minerals, and other chemical reactions. Modeling of such a complex storage and migration processes in general requires fine spatial and temporal discretization, and represents a large computational challenge, especially for site-scale models.

In this study, a large-scale numerical simulation of CO<sub>2</sub> geologic storage that predicts CO<sub>2</sub> migration and its impact on regional groundwater system was performed using parallel computing techniques. The simulation is designed for a preliminary investigation of industrial-scale CO<sub>2</sub> injection at the Tokyo Bay. The hydrogeological model covers an area about 60×70km<sup>2</sup> for the bay and surrounding area in the Kanto Plain. Thickness of the model layers is determined using data from a few dozen deep boreholes and several seismic reflection surveys. The model fully represents the whole hydrogeological system in the area, including surface topography, freshwater aquifers for drinking water, sealing layers, and CO<sub>2</sub> storage aquifers. The model domain is discretized into about 10 million gridblocks. Refined mesh is used in the vicinity of the assumed injection wells, located near the center of the model domain. To solve the high-resolution model efficiently, we used the parallelized multiphase flow simulator TOUGH2-MP (Zhang et al., 2008) with ECO2N (Pruess, 2005) fluid properties module of sub/supercritical CO<sub>2</sub> on a world-class high performance supercomputer in Japan, the Earth Simulator (with a total 5120 CPUs). The model will be used to simulate the hypothetical injection activities in the study area.

One of the primary goals of this study is to understand the behavior of CO<sub>2</sub> when it is stored in geological formations and its influence on regional groundwater system through the numerical model. Simulations are performed to determine the extent to which the CO<sub>2</sub> moves within the geological formations, and the range of possible pressure build-up in the local aquifers, and seepage changes on the land surface and sea floor in the study area. The results are important for assessing whether the sequestration will impair the geological integrity of the underground formations and whether CO<sub>2</sub> storage is secure and environmentally acceptable.

## **2. Massively Parallel Computation**

The simulations conducted in this study are computationally demanding because of the large grid size and the complex nonlinear processes involved. The ECO2N (Pruess, 2005) module of TOUGH2-MP (Zhang et al., 2007) is adopted for the simulations. TOUGH2-MP/ECO2N is an efficient parallel simulator for large-scale, long-term CO<sub>2</sub> geologic storage in saline aquifers, developed at Lawrence Berkeley National Laboratory. The parallel simulator is a three-dimensional, fully implicit model that solves large, sparse linear systems arising from discretization of the partial differential equations for mass and energy balance in porous and fractured media. The simulator is based on the ECO2N module of the TOUGH2 code and inherits all the process capabilities of the TOUGH2/ECO2N code, including a comprehensive description of the thermodynamics and thermophysical properties of H<sub>2</sub>O-NaCl-CO<sub>2</sub> mixtures, modeling single and/or two-phase isothermal or non-isothermal flow processes, two-phase mixtures, fluid phases appearing or disappearing, as well as salt precipitation or dissolution. TOUGH2-MP uses MPI for parallel implementation, the METIS software package (Karypis and Kumar, 1998) for simulation domain partitioning, and the iterative parallel linear solver package Aztec (Tuminaro et al., 1999) for solving linear equations by multiple processors.

The simulations are run on the Earth Simulator (ES), which is a high-speed supercomputer that was originally developed for, and greatly contributed to global climate change simulations. The ES had been the most powerful supercomputer in the world from 2002 to 2004. It consists of 640 nodes with eight vector processors and 16 GB of computer memory at each node, for a total of 5120 processors and 10 TB of main memory. The total peak performance is currently 40Tflop/s and is scheduled to increase to 131 Tflop/s by March 2009. In this study, TOUGH2-MP was ported to the Earth Simulator and successfully ran on it. The code was specially tuned up to increase its vector operation ratio (VOR) for the efficient use of the vector processors of the ES. The calculation time for the two-phase flow simulations with about 10 million gridblock models in this study was generally 1 to 2 days for 1000 year's simulation on 1024 processors.

## **3. Model Setup**

### *3.1. Modeling Area: Tokyo Bay and Kanto Plain*

The Kanto Plain (Figure 1a) is the largest coastal plain in Japan, surrounded by the Tokyo Bay, the Kanto Mountains, the Miura Peninsula, and the Boso Peninsula. The Tokyo Bay area is the most populated and industrialized area of Japan, where large stationary CO<sub>2</sub> emission sources, including coal-fired power, steel and cement plants, are located.

Annual emission of CO<sub>2</sub> from those large emission sources around the Tokyo Bay is about 100 MtCO<sub>2</sub>/year (RITE, 2006). Since 1950's, extensive explorative investigations and production of natural gas (mostly methane gas, dissolved in deep groundwater) have been carried out in the Boso Peninsula. The geologic structure in this area is well understood through dozens of deep borehole investigations and geophysical explorations for land subsidences and earthquakes (Suzuki, 2002; Sasaki et al., 2006). In recent years, a number of hot spring wells for spa resorts have been drilled to the depths over 1 km. A review work on deep groundwater and water quality in the area was conducted by Marui (2003). Due to these activities, relatively abundant geologic information is available for this area.

The plain is underlain by the Plio-Pleistocene Kanto sedimentary basin, composed of unconsolidated formations of silt, sand and gravel extending to a depth of more than 3,000 m. Figure 1b shows the conceptual geologic cross section across to a depth of around 4,000 m below the sea level. Primary geological formations at the site consist of the pre-Tertiary basement, the Tertiary Miura Group, the Plio-Pleistocene Kazusa Group, and the Pleistocene Shimosa Group. The Research Institute of Innovative Technology for the Earth, Japan (RITE, 2006) has investigated the possibility of CO<sub>2</sub> geologic storage in the middle or lower part of the Kazusa Group at depths greater than 800m, supposing sealing capabilities of the overlying upper Kazusa Group and Shimosa Group. If CO<sub>2</sub> is injected at the bottom of the basin under the Tokyo Bay, it may result in deep saline groundwater in the Kazusa Group being pushed up-dip into shallow aquifers, the buildup of groundwater pressures, and the change of water salinity of fresh water wells.

It should be emphasized that there is no plan of CO<sub>2</sub> geologic storage at the Tokyo Bay at present. We selected the Tokyo Bay area for the case study, because (1) the geologic data are relatively abundant in this area, and (2) the basin structure under the Kanto plain is suited for demonstrating the impact of down-dip CO<sub>2</sub> injection on near-surface (up-dip) aquifer.

### *3.2. Conceptual model and hydrogeologic settings*

A three-dimensional geological structure model was constructed for the 60km×70km modeling area centered on the Tokyo Bay as shown in Figure 1a. The surface topography are represented by 50m-grid DEM (digital elevation model) data published by the Geographical Survey Institute, Japan, and the formation boundaries are defined by 200m-grid DEM data by Sasaki et al. (2006). As an example, Figure 3 shows the contour map of bottom elevation of the Kazusa Group, obtained by interpolating formation boundaries identified by borehole loggings and seismic reflection surveys. The locations of boreholes and seismic survey lines used for the interpolation are also shown in the figure.

The geological model is discretized into IFDM (integral finite difference method) gridblocks for TOUGH2 simulations (see Figures 2 and 8), using the grid generation software VORLAY3D developed by Taisei Corporation. The 3D shapes of formation boundaries are represented explicitly as the interfaces between gridblocks. The horizontal surface is discretized by Voronoi polygons of about 250m resolutions. The Voronoi discretization allows varying spatial resolution at desired regions, such as the using of refined mesh in the vicinity of injection boreholes as shown in Figure 8. Discretization results in approximate 121,100 grids on each horizontal layer and 84 layers in the vertical direction with a total about 10 million gridblocks and 40 million connections between these gridblocks.

Table 1 lists the geological units/layers for Kazusa Group and the associated model hydrogeologic layers. These geologic formations have been organized into layered

hydrogeologic units based primarily on the sandy or muddy properties. The Kazusa Group is generally characterized by submarine sediment with thin-bedded sand-mud sequences. Thus, in the table, for example, 'muddy' represents a mud-dominated lithofacies, and is neither massive sand nor mud. In addition, the lithofacies in the Kazusa Group change rapidly in lateral directions. At present, the regional distribution of lithofacies has not been modeled. In this study, the simplified lithofacies of sand and mud for the Kazusa group are used, as shown in Table 1. In addition, perfect lateral continuities of all the model layers are assumed as illustrated in Figure 4.

According to the RITE report (2006), the middle part of the Kazusa Group, located at the depths of about 800m to 1000m below the ground surface, is selected as the target location for CO<sub>2</sub> injection. The selected storage formation, the Umegase (sandy) and Higashi-Higasa Formation (gravelly), is bounded at the top by a sealing layer, the Kokumoto Formation, followed by overlying sandy layers of the upper and middle part of the Kazusa Group, and the Shimosa Group. An additional sealing layer is assumed at the bottom of the Shimosa Group, based on the observations of pressure and salinity distributions that suggest the hydraulic communication between the Kazusa and Shimosa groups is weak (e.g., Nirei, 1988).

### *3.3 Boundary and Initial Conditions*

For this study, it is assumed that the CO<sub>2</sub> is injected through 10 wells in the bay, with annual rate of 1 MtCO<sub>2</sub>/year/well over 100 years, resulting in a total annual rate of 10 MtCO<sub>2</sub>/year. The simulation runs cover a time period of 1000 years including post-injection period of 900 years. Due to the variations in elevation and thickness of the model layers, the behavior of injected CO<sub>2</sub> will be affected by the variations in ambient temperature, salinity, and pressure, all of which influence the solubility of CO<sub>2</sub> in brine, as well as the density and viscosity of CO<sub>2</sub> and brine. The ambient conditions are used as the model initial conditions. A model run without CO<sub>2</sub> injection was carried out for steady state groundwater flow simulation to determine the pressure ambient conditions. Temperature varies linearly with depth, assuming geothermal gradient of 2°C per 100m depths and temperature of 15°C at the land surface. The salinity is assumed to be very low and no density-driven flow occurs. Geomechanical effects such as land-surface uplift are not explicitly considered.

Surface and side boundaries are hydraulically open, while the bottom is closed. The large lateral extent of the 60km × 70km model was chosen to ensure that the boundary conditions have minimal effect on the simulation results. At the lateral boundaries, the initial hydrostatic pressure is maintained and the boundaries are open for fluids to escape from or enter the model domain. The surface boundary is also open, so that the pressure is fixed to the atmospheric pressure. The bottom of the model is closed (no-flow) representing lower permeability of the Tertiary and pre-Tertiary basement rocks.

### *3.4 Model parameters and sensitivity cases*

The hydrogeologic parameters chosen for this study are given in Table 2. For simplification, in most simulation cases, all sandy and muddy layers have been assigned the same set of sand and mud properties, without variation with depth. Vertical/horizontal ratio of the permeabilities is assumed to be 1/10 in all the layers. Horizontal permeability is 100md for sandy layers and 1md for muddy layers in the base case. Porosity is set to 40%, based on well loggings and laboratory core test data. Rock compressibility is set to  $1 \times 10^{-9} \text{ Pa}^{-1}$  based on elastic modulus obtained from in-situ mechanical tests in this area.

Van Genuchten model is used to calculate the capillary pressure and relative permeability of the two-phase flow of CO<sub>2</sub> and water. The model parameters for capillary pressure and relative permeability calculation are basically employed from Pruess (2005), except for the residual water saturation for mud, which was increased from 20% to 40%. Parameters for base and sensitivity cases are summarized in Table 2. The first sensitivity case (case 2) increases/reduces pore compressibility of the base-case by one order of magnitude. In sensitivity cases 3 and 4, we change the permeabilities of the muddy seal layer in the Shimosa and Kazusa Group, respectively. In addition, the sensitivities of porosity and boundary condition are also explored in case 5 and 6.

## 4. Results and Discussion

### 4.1. Behavior of CO<sub>2</sub> plumes

Figure 5 shows the plan view of simulated distribution of CO<sub>2</sub> plumes from the 10 injection sites under the bay after 100-year injection for the base-case. The largest lateral plume appears in the injection layer as the buoyant CO<sub>2</sub> accumulating and spreading out under a less permeable muddy layer. Each plume extends a range around 4-5 km, which is about half distance away from the neighboring injection sites. The results indicate that the individual plumes from each injection sites have not merged after 100 year's injection. The evolution of CO<sub>2</sub> gas saturation for a plume on a cross-section is shown in Figure 6. After stop of the injection at 100 years, the plume slightly enters into the seal layer and moves to shallower part by its buoyancy force, but basically continues to be contained under the sealing layer. As shown in Figure 7, initially injected CO<sub>2</sub> is mostly stored as supercritical fluid. However, after the termination of the injection, the contribution of dissolution in groundwater gradually increases and finally becomes dominant.

### 4.2. Impact on regional groundwater flow

#### 4.2.1. Pressure buildup

Pressure buildup at the injection points is about 20 bars. Figure 8 shows spatial distribution of calculated hydraulic heads from the base case at (a) pre-injection and at (b) 100 years, showing that the pressure buildup can occur over a wide area of the region. Even though the extent of CO<sub>2</sub> plumes is relatively small, the range of influence area of pressure buildup caused by CO<sub>2</sub> injection and storage is much larger. Pressure buildup propagates away from injection wells in a much fast speed than migration of CO<sub>2</sub> plumes. At time 100 years, a merged high pressure buildup region has evolved in the center of injection area. The pressure buildup reaches maximum value at 100 years and recovers right after stop of the injection.

Time evolutions of simulated pressure buildup at the depths of 50m, 100m, 200m, and 300m at several observation locations around the Tokyo Bay are shown in Figure 9a. Note that these locations are urban inlands with few tens of kilometers away from the injection points. Figure 9a indicates that the pressure recovery takes almost the same time period as the buildup. Significant buildup of 1-1.5 bar is seen at 300m depths of the point C and G, while it is negligibly small at the point A due to absence of top sealing layer and the relatively larger distance from injection points. The pressure change at a given site is a superposition of pressure responses from the closest injection well as well as from other nearby injection wells, whose radius of influence is larger than the distance of observation location to the wells. Figure 9b shows vertical-pressure profiles for the observation point A and G at the time of 100 years. From this figure, it is clear the

shallow seal layer, assumed at the bottom of Shimosa Group, plays a key role for pressure change at point G. This result suggests that significant pressure buildup can occur in a confined aquifer even at less depth.

For the sensitivity cases, comparison of pressure buildup at 300m depths of point G is shown in Figure 10. As expected, the larger the pore compressibility is, the slower the pressure buildup, and the longer the recovery time (Figure 10a). In the current model, the permeability of seal layer is the most important factor that influences the pressure buildup as seen in Figure 10b. For example, by lowering the permeability of shallow seal layer in the Shimosa Group by one order (case 3b), pressure buildup is almost twice of the base case, suggesting the importance of investigations on hydrogeological layers and flow parameters even in shallower depths. Figure 10c indicates decrease of porosity for the storage and seal layers causes higher pressure buildup. This attributes to reduce of pore space for CO<sub>2</sub> storage. As also shown in Figure 10c, side boundary condition has minor effects to pressure perturbation in the current settings and scale of the model.

#### *4.2.2. Discharge/recharge area*

Due to the large-scale CO<sub>2</sub> injection activity, it is expected that a large volume of groundwater is pushed out and discharged on the land surface. Figure 11 shows the distribution of groundwater discharge or recharge rate on the surface. The change in discharge/recharge rate from the initial condition is shown in Figure 11b. The discharge increase mainly occurs in seabed, so that its impact on the land surface area is relatively small. Significant increase is also found along the boundary of the Shimosa and Kazusa Group, indicated in the figure as a white line. The increase of the discharge is in the order of few tens of mm/year as local maximum, which is about 1% of annual precipitation of the Kanto area (about 1400mm/year) and is smaller than annual variation levels. Dividing the discharge rate by porosity gives a rough estimation of transport velocity of groundwater in vertical direction near the surface. For example, with a discharge rate of 20 mm/year and 40% porosity, a flow velocity of 0.02m/year can be obtained, which is slower than the estimated rate in the natural groundwater at Alberta Basin (i.e., 0.1 to 1m /year; Bachu et al. [1994]).

## **5. Concluding Remarks**

The massively parallel computing technique makes it possible to perform comprehensive simulations that predict not only CO<sub>2</sub> migration but also its impact on regional groundwater system. It was successfully demonstrated that the Earth Simulator efficiently solved the two-phase flow model with more ten million gridblocks, one of the largest CO<sub>2</sub> sequestration model ever reported. The simulation runs for 1000 years period were finished within 1-2 day/run with 1024 processors. The high-resolution model could be useful to depict three-dimensional region of influence during/after injection of CO<sub>2</sub> and the possible implications for shallow groundwater resources.

In terms of the impact of CO<sub>2</sub> geologic storage on groundwater flow that was hypothetically simulated at the Tokyo Bay, following implications were obtained. (1) The CO<sub>2</sub> plumes can spread out a range of several kilometers within 100 year's injection using the investigated injection schemes. (2) Build-up of groundwater pressure in shallow confined layers can occur in extensive regions including urban inlands. (3) Groundwater discharge to the land surface and seabed can increase in the order of few tens of mm/year

due to the injection activities. Sensitivity studies indicate that the permeability of sealing layers and storage layer is one of the most important parameters that influence the performance of CO<sub>2</sub> sequestration on the regional groundwater system. In addition, porosity and compressibility are also sensitive to the system pressure buildup. Besides the improvement of this preliminary hydrogeological model, the investigation of the effect of fault and abandoned and existing wells will be future addressed.

### **Acknowledgement**

We greatly appreciate Satoshi Imamura, Tomoyuki Aoki, and Toyokazu Ogawa at Taisei Corporation, Karsten Pruess at Lawrence Berkeley National Laboratory for encouragement and helpful discussions. Our sincere thanks also to Satoru Shingu and Yuichi Hirokawa at Japan Agency for Marine-Earth Science and Technology (JAMSTEC) and Takaaki Noguchi at NEC system technologies Ltd. for their extensive helps and support for the use of the Earth Simulator. The authors wish to thank to Katsuji Sasaki and Akira Hyuuga at Suncoh Consultant Inc for providing us the digital data set of geological formations of the Kanto Plain. The use of the Earth Simulator was supported by “Open Advanced Facilities Initiative for Innovation (Strategic Use by Industry)” funded by Ministry of Education, Culture, Sports, Science and Technology (MEXT) of Japan. This work was also partially supported by the U.S. Department of Energy under Contract No. DE-AC02-05CH11231.

### **References**

- Bachu, S., Gunter, W.D., Perkins, E.H., 1994. Aquifer disposal of CO<sub>2</sub>: hydrodynamic and mineral trapping. *Energy Convers. Manage.*, Vol. 35, No.4, pp. 269-279.
- Birkholzer, J. T., Zhou, Q., Tsang, C.F., 2008. Large-scale impact of CO<sub>2</sub> storage in deep saline aquifers: A sensitivity study on pressure response in stratified systems, *Int. J. Greenhouse Gas Control* (in press)
- Doughty, C., Pruess, K., 2003. Modeling supercritical carbon dioxide injection in heterogeneous porous media, *Vadose Zone Journal* 3: 837-847.
- Ghomian, Y., Gary, P.A., Sepehrnoori, K., 2008. Reservoir simulation of CO<sub>2</sub> sequestration pilot in Frio brine formation, USA Gulf Coast. *Energy* 33, 1055-1067
- Karypsis, G. And Kumar, V., 1998. METIS: A Software Package for Partitioning Unstructured Graphs, Partitioning Meshes, and Computing Fill-Reducing Orderings of Sparse Matrices, V4.0, Technical Report, Department of Computer Science, University of Minnesota.
- Marui, A., 2003. Deep groundwater in the Kanto Plain, *J. Japan. Assoc. of Hydrol. Sci.*, Vol. 33, No. 3, pp.149-160.
- Nicot, J. P., 2007. Evaluation of large-scale CO<sub>2</sub> storage on fresh-water sections of



- aquifers: An example from the Texas Gulf Coast Basin, *Int. J. Greenhouse Gas Control*, 2, pp. 582-593.
- Nirei, H., 1988. Kanto sedimentary basins -fluid resources in underground and regional groundwater flow-, *Urban Kubota*, Vol. 18, pp.45-50 (in Japanese).
- Pruess, K., 2005. ECO2N: A TOUGH2 Fluid Property Module for Mixtures of Water, NaCl, and CO<sub>2</sub>, Lawrence Berkeley National Laboratory Report, LBNL-57952.
- Sasaki, K., T. Hyuga, S. Nakamura, S. Horikawa, A. Marui, A. Miyakoshi, 2006. Stratigraphy of deep aquifer in the eastern Tokyo Bay area, *Proceedings of 2006 Spring Meeting of Japanese Association of Groundwater Hydrology*, pp.80-85 (in Japanese).
- Suzuki, H., 2002. Underground Geological Structure beneath the Kanto Plain, Japan, *Report of the National Research Institute for Earth Science and Disaster Prevention*, Vol. 63, pp.1-19 (in Japanese)
- The Research Institute of Innovative Technology for the Earth (RITE), 2006. Research and development of underground technology for carbon dioxide, *Research report*. (in Japanese)
- Tuminaro, R.S., Heroux, M., Hutchinson, S.A. and Shadid, J.N., 1999. Official Aztec user's guide, Ver 2.1, Massively Parallel Computing Research Laboratory, Sandia National Laboratories, Albuquerque, NM.
- Yamamoto, H., K. Zhang, K. Karasaki, A. Marui, 2007. Massively Parallel Computing System for Geologic Storage of CO<sub>2</sub>, *Taisei Technology Center Report*, No.40, pp.41-1-10 (in Japanese with English abstract).
- Zhang, K., C. Doughty, Y.S. Wu, K. Pruess, 2007. Efficient Parallel Simulation of CO<sub>2</sub> Geologic Sequestration in Saline Aquifers, *SPE* 106026.
- Zhang, K., Y.S. Wu, and K. Pruess, 2008. User's Guide for TOUGH2-MP -. A Massively Parallel Version of the TOUGH2 Code, LBNL-315E, Lawrence Berkeley National Laboratory Report.

Table 1. Lithofacies of the Kazusa Group (a) Lithofacies (modified from Sasaki et al., [2006]); (b) Conceptual hydrogeological model

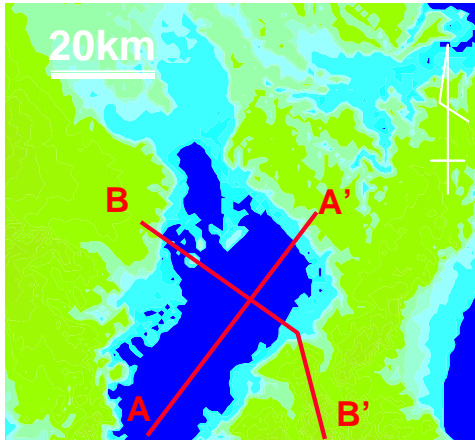
Age		Ma	Group/Formation	Lithofacies West/East				
Quaternary	Holocene		fluvial/river terrace sediments	-				
			Shimoso Group	-				
	Pleistocene	Late	0.6	Kazusa Group	Upper	Kongochi	sandy	
						Upper Kasamori	muddy sandy	
		Lower Kasamori				gravelly		
		Chonan				sandy		
	Ichijyuku	gravelly sandy						
	Middle	Early			0.8	Lower	Kokumoto	muddy
							Umegase	sandy
							Higashi Higasa	gravelly
Neocene	Pliocene	1.0			Lower	Tomiya	muddy	
								1.2
			Namihana					
			Katsuura					
Miocene		1.7	Kurotaki	gravelly	-			
						Awa Group	-	-

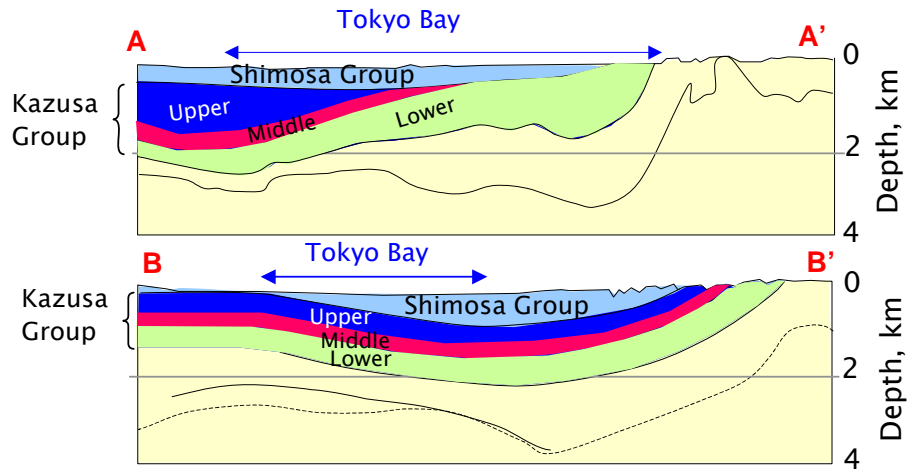
Age		Ma	Group/Formation	Lithofacies West/East			
Quaternary	Holocene		fluvial/river terrace	Sandy			
			Shimoso	Sandy	Muddy		
	Pleistocene	Late	0.6	Kazusa Group	Upper	Upper Kazusa	Sandy
						Middle	Early
		1.0			Lower		
						1.2	Lower Kazusa
Miocene		1.7	Kurotaki	Sandy			
				Awa Group	-		

Table 2. Model parameters for base and sensitivity cases (changes from the base-case are highlighted)

	Case	Pore Compressibility (Pa <sup>-1</sup> )	Permeability (md)				Porosity (%)	Side Boundary (Open/Close)
			Shimosa Group		Kazusa Group			
			Sandy	Muddy	Sandy	Muddy		
Base case	1	1×10 <sup>9</sup>	100	1	100	1	40	Open
Pore Compressibility	2a	1×10 <sup>8</sup>	100	1	100	1	40	Open
	2b	1×10 <sup>10</sup>	100	1	100	1	40	Open
Shimosa Seal permeability	3a	1×10 <sup>9</sup>	100	10	100	1	40	Open
	3b	1×10 <sup>9</sup>	100	0.1	100	1	40	Open
Kazusa Seal permeability	4a	1×10 <sup>9</sup>	100	1	100	10	40	Open
	4b	1×10 <sup>9</sup>	100	1	100	0.1	40	Open
Porosity	5	1×10 <sup>9</sup>	100	1	100	1	20	Open
Boundary Condition	6	1×10 <sup>9</sup>	100	1	100	1	40	Close



(a) Topographic map showing the cross sections.



(b) Geologic cross section

Figure 1. Topographic map and geologic cross section around the Tokyo Bay (RITE [2006])

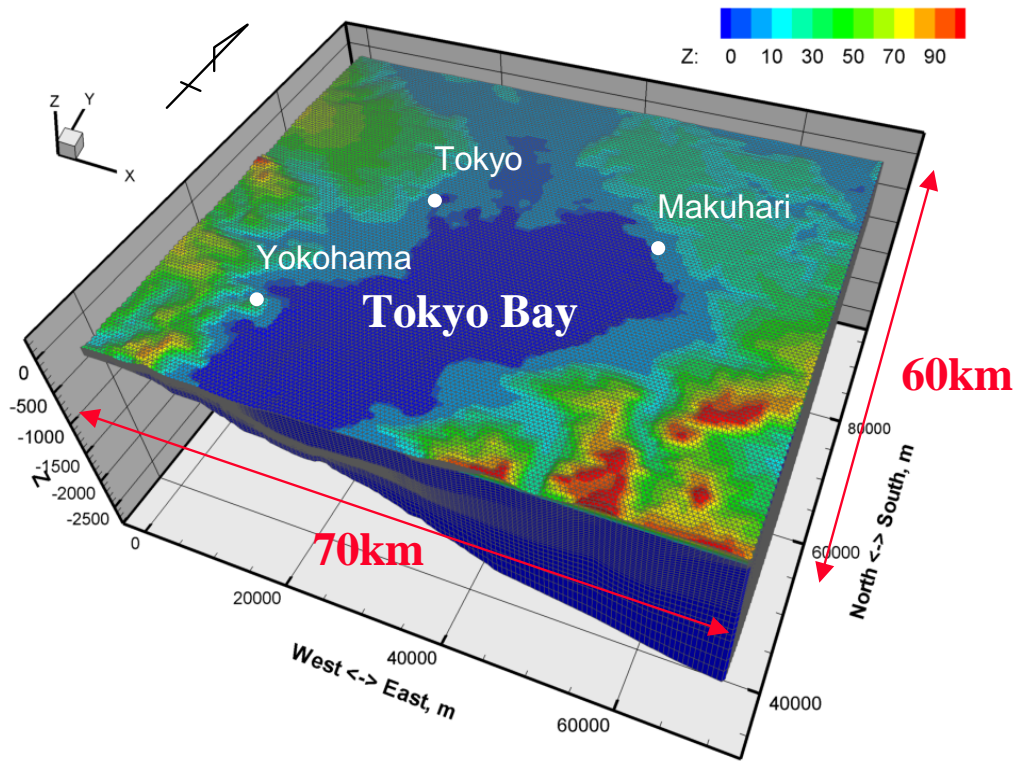


Figure 2. Three-dimensional model domain.

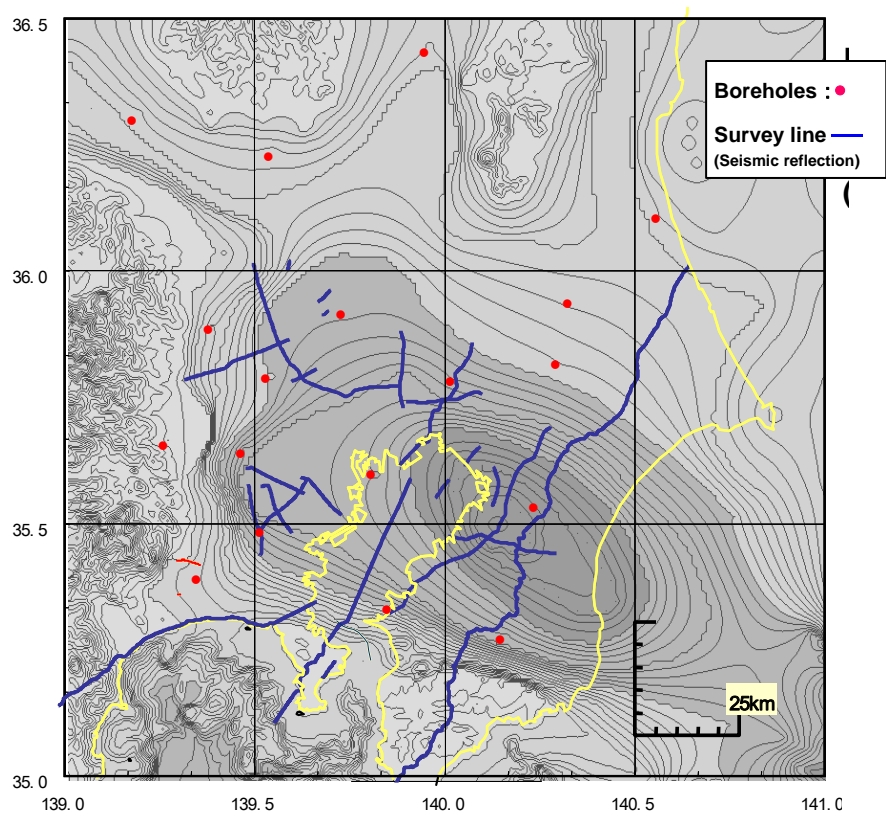


Figure 3. Bottom elevations of the Kazusa Group (Sasaki, et al., 2006)

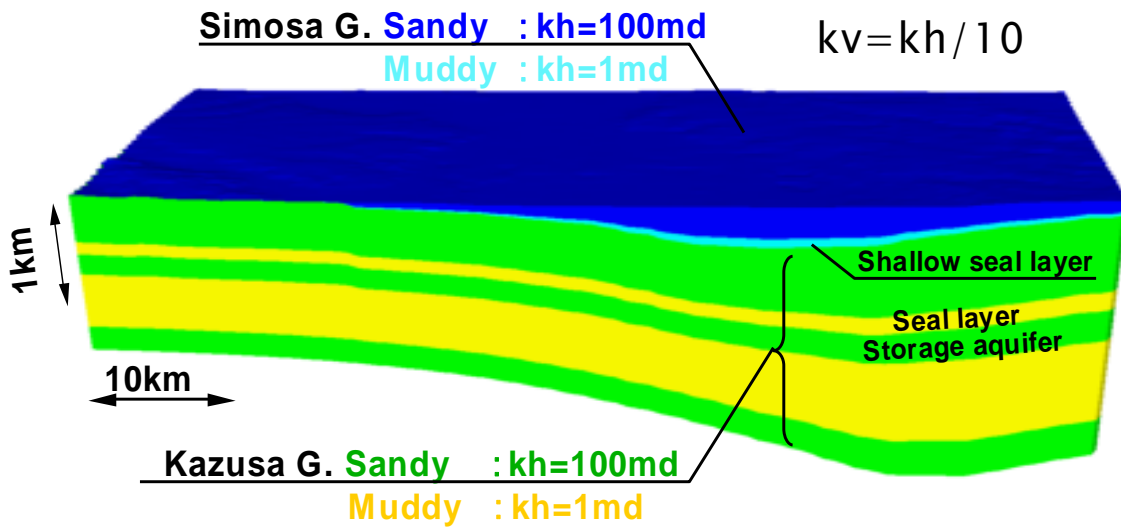
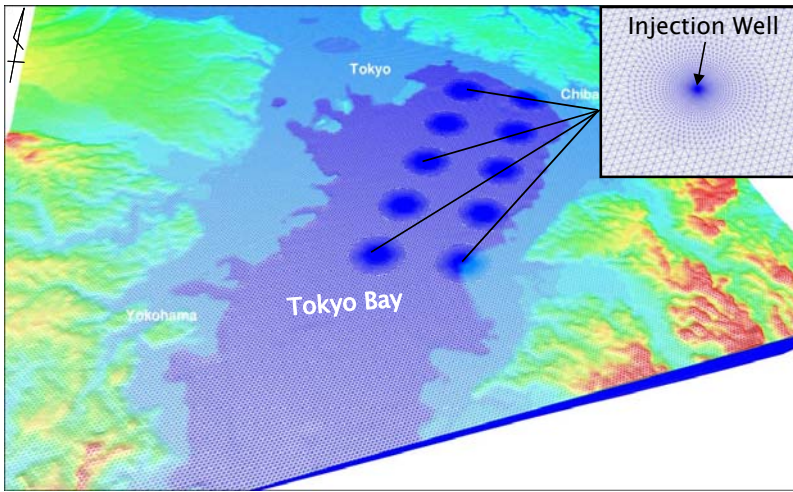
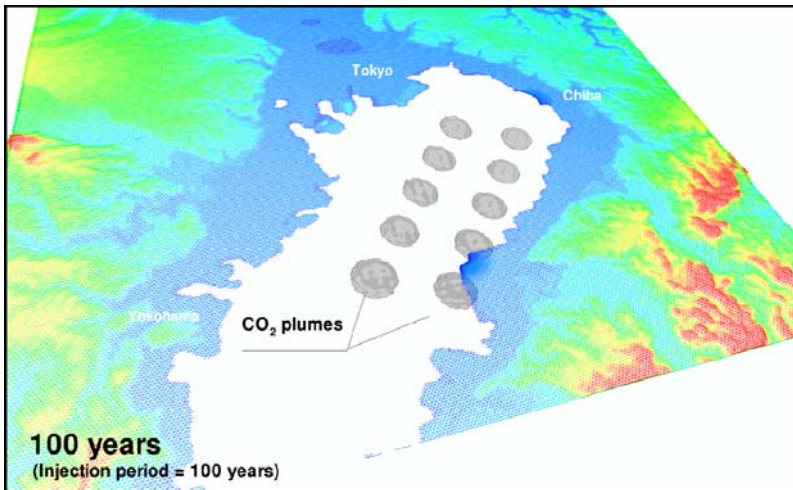


Figure 4. Hydrogeological model layers (base case)



(a) Numerical meshes (about 10 million gridblocks)



(b) Simulated CO<sub>2</sub> plumes (at 100 years)

Figure 5. Model mesh showing grid refinement around the injection wells and simulated CO<sub>2</sub> plumes (base-case)



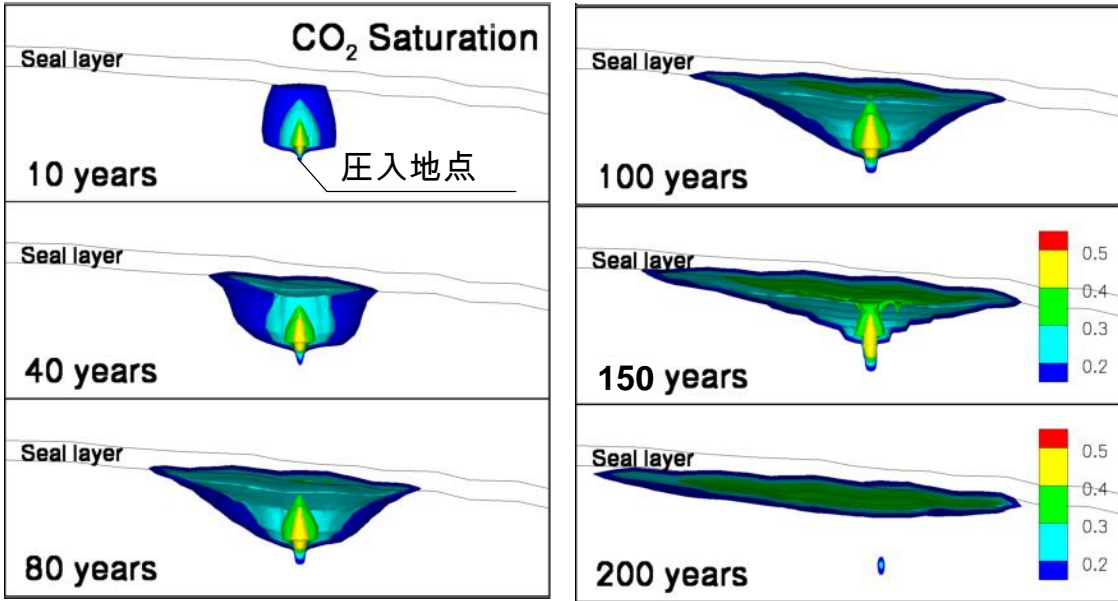


Figure 6. Evolution of CO<sub>2</sub> plume during and post injection (base-case)

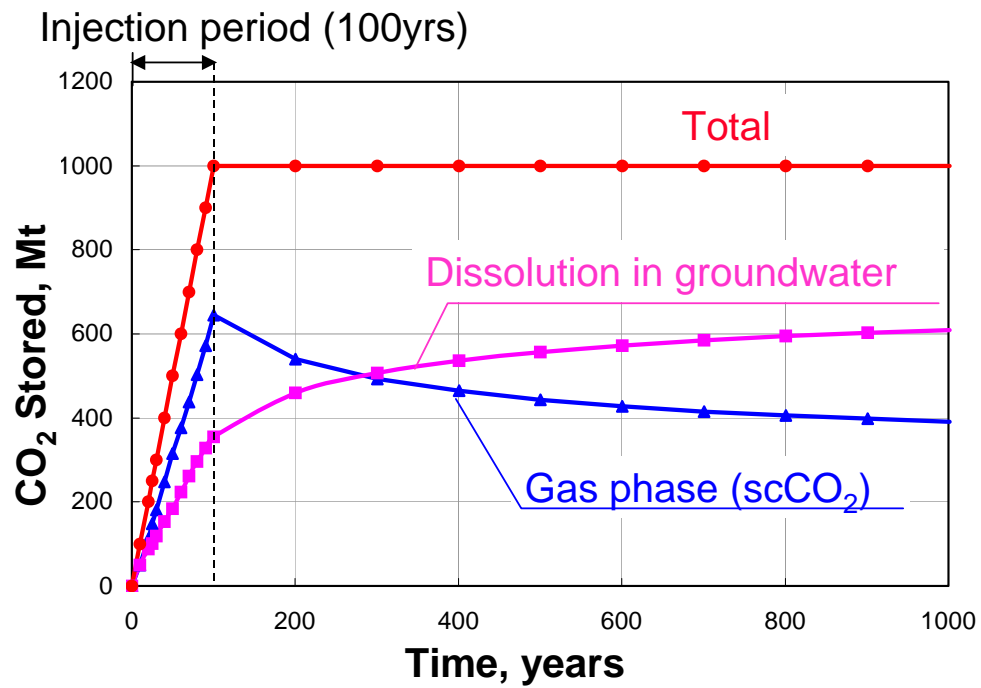
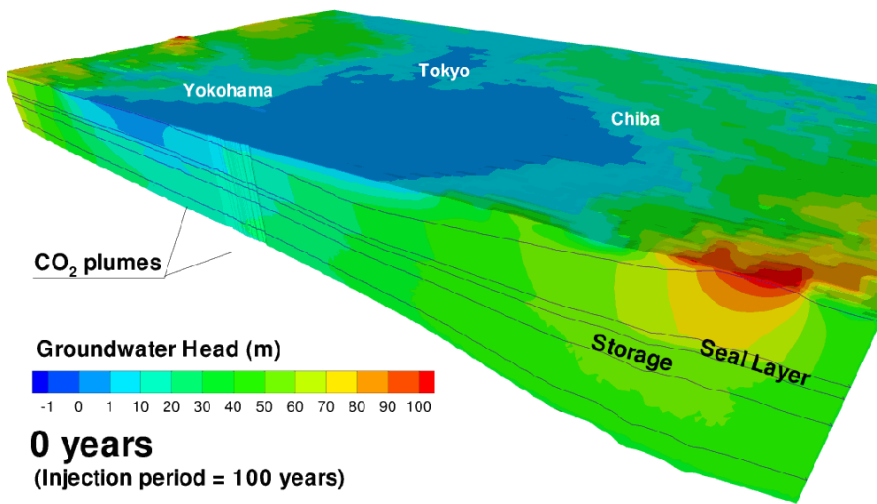
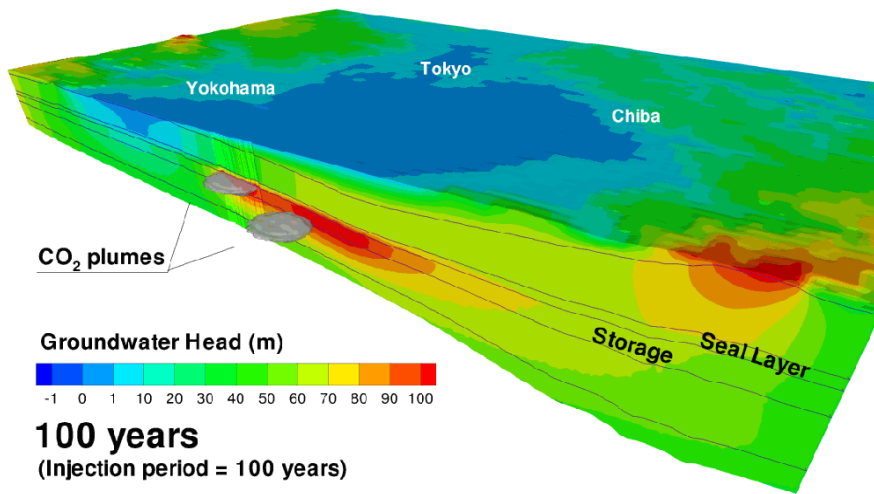


Figure 7. CO<sub>2</sub> partitioning among dissolution and gas phase in the storage aquifers (base-case)

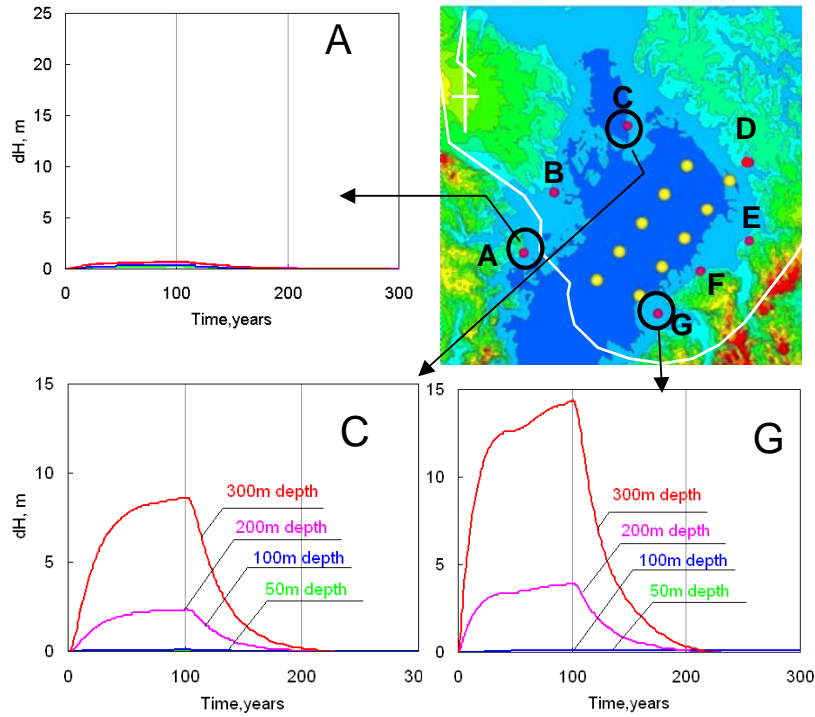


(a) Initial condition (ambient groundwater pressure distribution)

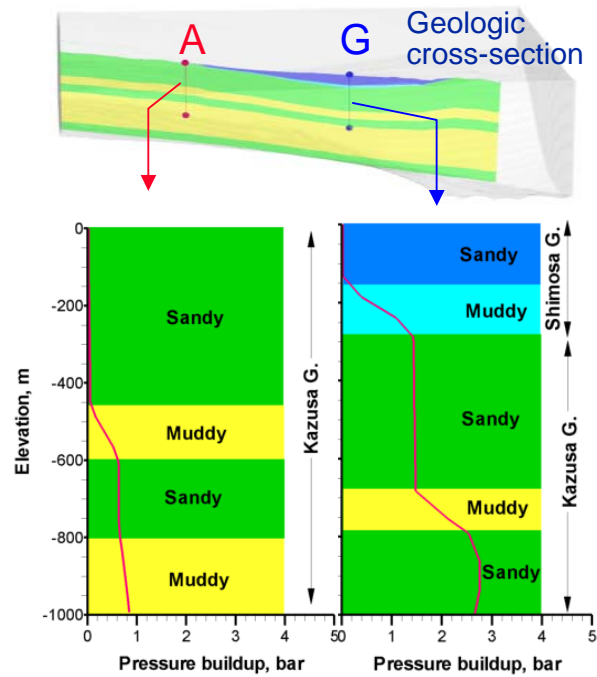


(b) After 100 years injection

Figure 8. Regional groundwater head change due to CO<sub>2</sub> injection (base case)



(a) Groundwater head change with time



(b) Groundwater head change with depth

Figure 9. Changes in groundwater heads /pressures after CO<sub>2</sub> injection (base-case)

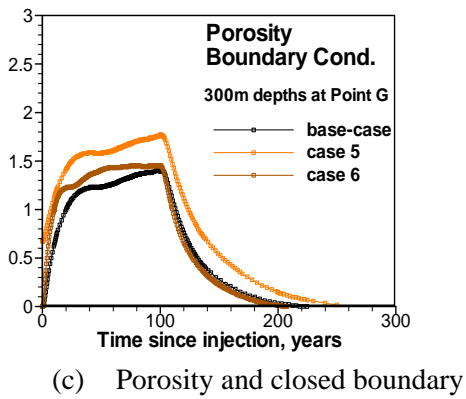
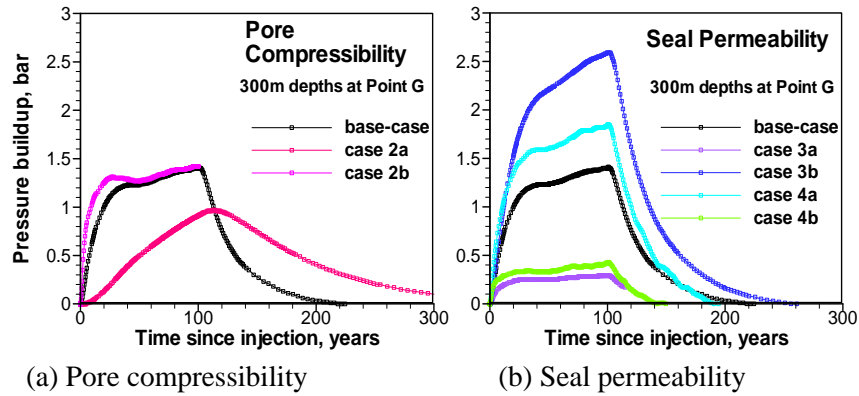
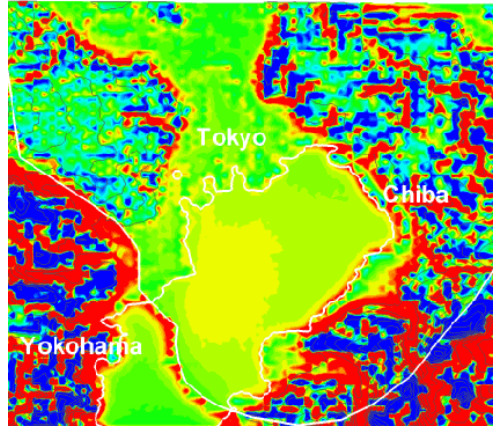


Figure 10. Comparison of pressure buildups in the sensitivity cases (at 300 m depth at point G)



(a) Surface groundwater discharge / recharge rate at 100 years

(b) Increase of discharge rate to the surface at 100 years

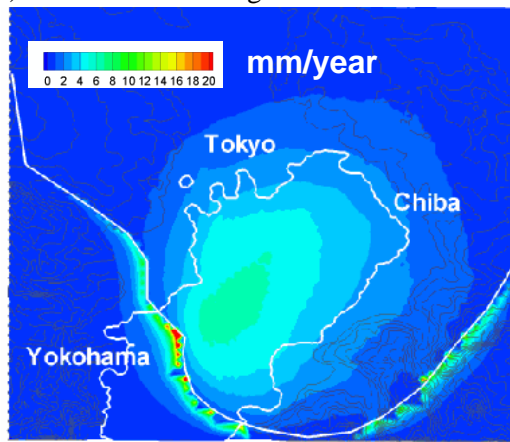


Figure 11. Change in surface groundwater discharge due to CO<sub>2</sub> storage (at 100 years, base-case)